Journal of Multidisciplinary Engineering Science and Technology (JMEST)
ISSN: 2458-9403
Vol. 12 Issue 12, December - 2025

Antitumor Efficacy of the Resveratrol Analogue AR26 in Aggressive Melanoma Models

Ana Paula Guarnieri Almeida[1]*, Letícia Gomes de Oliveira[1]*, Danielle Cristina Zimmermman-Franco[1], Lívia Bittencourt dos Reis[1], Luiza Gabriele Lima Pereira[1], Raíssa Soares Meinel[2], Adilson David Da Silva[3], Gilson Costa Macedo[1].

[1]Centro de Tecnologia Celular e Imunologia Aplicada (IMUNOCET), Instituto de Ciências Biológicas, Universidade Federal de Juiz de Fora, Juiz de Fora, MG, Brazil. [2]Laboratório de Estrutura e Função de Proteínas, Instituto de Ciências Biológicas, Universidade Federal de Juiz de Fora, Juiz de Fora, MG, Brazil. [3]Departamento de Química, Instituto de Ciências Exatas, Universidade Federal de Juiz de Fora, Juiz de Fora, MG, Brazil. *These authors contributed equally to this work

e-mail address: gilson.macedo@ufjf.br

***Abstract*— Melanoma remains one of the most aggressive skin cancers, and the limited efficacy and toxicity of current therapies highlight the need for safer and more effective antitumor agents. Resveratrol is widely recognized for its antitumor properties, but its therapeutic potential is restricted by poor bioavailability and chemical instability. In this study, we evaluated AR26, a synthetic analogue of resveratrol, in murine and human melanoma models using two-dimensional (2D) cultures and three-dimensional (3D) spheroids. AR26 demonstrated moderate acute cytotoxicity against melanoma cells, but exhibited a markedly superior biocompatibility profile compared with resveratrol in HaCaT keratinocytes and L929 fibroblasts. At its minimum effective concentration, AR26 significantly inhibited melanoma cell migration and sustained proliferation suppression for up to 72 hours, outperforming resveratrol in long-term assays. In human spheroids, AR26 did not reduce spheroid size but conferred a strong and persistent inhibition of post-treatment migratory outgrowth, whereas resveratrol showed no significant effect. These results indicate that AR26 modulates key hallmarks of tumor progression and exerts durable biological effects after drug withdrawal. Collectively, the findings support AR26 as a promising candidate for further preclinical development against metastatic melanoma.**

Keywords — Melanoma, Resveratrol Analogue, AR26, Cell Migration, Tumor Spheroids, Proliferation Inhibition, Cytotoxicity

I. INTRODUCTION

Cancer represents one of the most critical public health challenges of the 21st century, accounting for approximately one in six deaths globally. Beyond its high mortality, the disease imposes a profound societal and economic burden, with incidence rates projected to rise sharply in the coming decades [1-3]. Cancer treatment is complex and determined by multiple factors. While conventional therapies such as surgery, chemotherapy, and radiotherapy remain the mainstay of oncology, their effectiveness is often limited by resistance and severe adverse effects that compromise patient quality of life [4–8]. Even with the advent of immunotherapy and targeted therapies, the escalating global burden highlights the urgent need for safer and more effective treatment strategies [9].

Natural bioactive products have emerged as a prominent focus in cancer research due to their demonstrated antitumor activities and relatively low toxicity profiles when compared to conventional chemotherapeutics [10]. Among them, resveratrol (RVT - 3,4',5-trihydroxy-trans-stilbene), a naturally occurring phytoalexin found in medicinal plants, grape skin, peanuts, and red wine [11], has garnered substantial interest for its diverse biological effects, including antioxidant, anti-inflammatory, and notable antitumor properties [11-21].

In the context of cancer, resveratrol has been shown to act as a chemopreventive agent, modulating multiple stages of carcinogenesis: initiation, promotion, progression, and metastasis [22]. Furthermore, it exerts therapeutic potential across a broad spectrum of malignancies, including prostate and colorectal cancers [23], as well as in lung [24], breast [25–27], and skin tumors [28–30]. In addition, resveratrol enhances the antitumor activities of commercial drugs such as Melphalan [31], Herceptin [32], and Tamoxifen [33].

Despite these benefits, RVT's clinical application is severely limited by its poor bioavailability and rapid metabolism [34]. To address these limitations, several studies have focused on the synthesis of structural analogues with improved pharmacokinetic profiles, while preserving the desirable bioactivities of the parent compound [35,36].

In the present study, we evaluated the antitumor activity of AR26, a synthetic resveratrol analogue, against relevant melanoma models. Previous work from our group established that AR26 exhibits low *in*

vitro toxicity for immune cells while possessing potent antioxidant and anti-inflammatory properties [35], characteristics associated with tumor suppression. Unlike previous research that has often focused on acute cytotoxic potency, we hypothesized that strategic molecular modifications could yield a compound with superior efficacy in suppressing the complex, long-term cellular programs that drive tumor aggressiveness and metastasis. Here, we demonstrate that AR26 inhibits key hallmarks of tumor progression, positioning it as a candidate for further therapeutic development.

II. Material and Methods

A. General procedures

The compound AR26 (C14H11NO3) was synthesized following the protocol previously described in [37]. Briefly, the analogue was obtained by condensation of 2-hydroxyaniline with an equimolar amount of the corresponding aromatic aldehyde in ethanol at room temperature. The resulting solid was isolated by filtration, washed with ethanol, and dried in an oven (yield 78%).

The compound was characterized via one-dimensional nuclear magnetic resonance (1D-NMR) and melting point. The data obtained were consistent with previously reported literature values [35, 37].

All reagents and solvents were purchased from commercial suppliers and used without further purification. Analytical reagent grade chemicals were employed throughout. Resveratrol, used as a reference compound, was obtained from Fagron (São Paulo, SP, Brazil), with a stated purity of 99%.

For biological assays, the compound was dissolved in ethanol and subsequently diluted in the appropriate culture medium. The final ethanol concentration to which the cells were exposed did not exceed 0.2% (v/v). A corresponding vehicle control was included in all assays and showed no statistically significant difference from the untreated control group.

B. Cell Culture

The B16-F10 murine melanoma cell line (RRID:CVCL_0159) and the HaCaT human epidermal keratinocyte cell line (RRID:CVCL_0038) were kindly provided by Dr. Guilherme Diniz Tavares from the Laboratory of Nanostructured System Development, Federal University of Juiz de Fora (UFJF), Brazil. The L929 murine fibroblast (RRID:CVCL_0462) and SK-MEL-28 human melanoma (RRID:CVCL_0526) cell lines were obtained from the cell bank of the IMUNOCET Laboratory (UFJF), Brazil.

Cells were routinely maintained in RPMI-1640 medium (Gibco) for L929, and in DMEM (Gibco) for B16-F10, HaCaT, and SK-MEL-28 cells. All media were supplemented with 10% fetal bovine serum (FBS, Gibco), 1% streptomycin, and 100 U/mL penicillin (Gibco), and cells were incubated at 37 °C in a humidified atmosphere containing 5% CO_2 until use.

C. Cell Viability Assay

The viability of cells was evaluated using the MTT (3-(4,5-dimethylthiazol-2-yl)-2,5-diphenyltetrazolium bromide) reduction assay, following the ISO 10993-5:2009 guidelines. Briefly, cells were seeded into 96-well plates (1×10^4 cells/well), incubated for 24 h, and then treated with resveratrol or AR26 at varying concentrations for an additional 24 h (0-800 µM).

At the end of the treatment period, the MTT solution (0.5 mg/mL - Invitrogen) was added to each well, and plates were incubated for 2 h (37°C, 5% CO_2). The supernatant was then carefully removed, and the resulting formazan crystals were solubilized in DMSO (100 µL/well). Absorbance was measured at 595 nm using a microplate spectrophotometer (SpectraMax M2, Molecular Devices, CA, USA). Cell viability was expressed as a percentage relative to untreated control cells (set as 100% viability). IC_{50} values (the concentration required to reduce cell viability by 50%) were calculated using nonlinear regression analysis (log[inhibitor] vs. normalized response, variable slope) in GraphPad Prism software (version 8.0.1, GraphPad Software, San Diego, CA, USA).

D. Cell Proliferation

Cell proliferation was assessed in B16-F10 and SK-MEL-28 cell lines using the CellTrace™ CFSE Cell Proliferation Kit (Invitrogen, Thermo Fisher Scientific, Waltham, MA, USA), following the manufacturer's protocol. Briefly, cells were harvested during the logarithmic growth phase, washed twice with phosphate-buffered saline (PBS), and resuspended at a concentration of 5×10^6 cells/mL in PBS containing 5 µM CFSE. Cells were incubated at room temperature for 10 minutes in the dark. The labeling reaction was quenched by the addition of five volumes of cold complete culture medium (medium supplemented with 10% fetal bovine serum), and cells were incubated on ice for 5 minutes. Subsequently, cells were washed twice with complete medium to remove excess dye. To ensure initial fluorescence homogeneity across all experimental groups, this staining procedure was performed in a single cell suspension prior to seeding into treatment wells.

Labeled cells were seeded into 24-well plates at a density of 2×10^5 cells/well and incubated at 37°C in a humidified atmosphere with 5% CO_2. After 24 hours, cells were treated with RVT (50 µM) or AR26 (100 µM). Cells were harvested at 24-, 48-, and 72-hours post-treatment, washed with PBS containing 1% FBS, and analyzed by flow cytometry using a CytoFLEX system (Beckman Coulter, CA, USA) equipped with a 488 nm excitation laser and a 525/40 nm emission filter to detect CFSE fluorescence.

Data were analyzed using FlowJo software (version X.0.7, Tree Star Inc.). The dilution of CFSE fluorescence intensity was used to determine the extent of cell proliferation, expressed as mean fluorescence intensity (MFI). Unstained cells and

CFSE-labeled untreated cells were included as controls.

E. Cell migration

Cell migration was assessed using a wound healing (scratch) assay. Briefly, B16-F10 or SK-MEL-28 cells were cultured as previously described until the logarithmic growth phase. For the assay, cells were seeded in 24-well plates at 1.5×10^5 cells per well to achieve a confluent monolayer within 24 h. A linear scratch was created in each well using a sterile 200 µL pipette tip, and wells were gently washed with PBS to remove detached cells. Cells were then treated with AR26 (100 µM) or RVT (50 µM) and cultured for 24 h in complete medium containing 0.5% FBS.

Migration into the wound area was monitored at 0h and 24 h using phase-contrast microscopy. Three images were captured per well at different sequential locations, using marked reference points on the plate. Wound closure was quantified using ImageJ (National Institutes of Health, Bethesda, MD, USA) with the MRI Wound Healing Tool plugin, and results were expressed as the percentage of wound closure relative to the initial scratch area. All experiments were performed in quadruplicate and independently repeated at least twice.

F. Tumor Spheroids and Spheroid Migration Assay

Human SK-MEL-28 cells were initially cultured as monolayers (2D), as previously described, and subsequently adapted to three-dimensional (3D) culture. To generate spheroids, monolayer cells were dissociated with trypsin/EDTA (Gibco) and plated at a density of 6,000 cells per well in 96-well U-bottom plates (Sarstedt, Nümbrecht, Germany) previously coated with 1% agarose. The cells were then cultured for 5 days under standard conditions (37°C, 5% CO_2) in complete DMEM to promote spheroid formation.

For the growth assay, established spheroids were treated with AR26 or resveratrol (RVT) at the indicated concentrations for 72 h. During this treatment period, spheroid integrity and diameter were monitored at 0, 24, 48, and 72 h via phase-contrast microscopy to assess the direct effects of the compounds on spheroid growth. Vehicle-treated spheroids (0.1% ethanol) served as the control.

To subsequently assess cell migration, the same spheroids were collected at the end of the 72-h treatment period, washed with PBS, and individually transferred to new 24-well adherent plates containing fresh, compound-free medium. The ability of the cells to migrate away from the spheroid was then monitored daily. The total area of migrated cells was quantified over time from phase-contrast images using ImageJ software (National Institutes of Health, Bethesda, MD, USA).

G. Statistical analysis

Data were analyzed using GraphPad Prism version 8.0.1 (GraphPad Software, San Diego, CA, USA). Results were expressed as mean ± standard deviation (SD). Statistical comparisons were performed using one-way or two-way analysis of variance (ANOVA), as appropriate, followed by Tukey's post hoc test. Differences were considered statistically significant at $p < 0.05$.

III. RESULTS AND DISCUSSION

A. AR26 demonstrates moderate cytotoxicity against melanoma cells but a superior biocompatibility profile in vitro

The evaluation of acute cytotoxic potential is a fundamental first step in the development of new anti-tumor agents. In this study, we assessed the effects of the resveratrol analogue AR26 on the viability of B16-F10 (murine melanoma) and SK-MEL-28 (human melanoma) cell lines. Cells were exposed to increasing concentrations of each compound (0–800 µM) for 24 hours, and viability was measured by MTT.

As shown in Figure 1A, both compounds exhibited comparable cytotoxicity against B16-F10 melanoma cells. A significant reduction in cell viability was observed for both AR26 and RVT at concentrations starting from 50 µM. This similar potency was confirmed by their calculated IC50 values, which were nearly identical at 194.9 ± 14.7 µM for AR26 and 186.5 ± 10.6 µM for RVT. In contrast, a difference in potency was observed in the SK-MEL-28 cell line (Fig. 1B). RVT was more potent, significantly reducing tumor cell viability at concentrations starting from 50 µM (IC50 = 145.0 ± 7.7 µM). AR26, however, showed a weaker effect on this line, only achieving a significant reduction in viability at concentrations of 100 µM and above (IC50 = 728.9 ± 45.2 µM).

While the antitumor potency of AR26 appeared moderate compared to RVT in human cells, a striking advantage emerged in biocompatibility assays performed in accordance with the ISO 10993-5:2009 standard (Fig. 1C, D). In human keratinocytes (HaCaT), AR26 did not significantly impact viability at concentrations below 100 µM. Furthermore, at 200 µM, AR26 maintained cell viability near 90% (89.1%), and its calculated IC50 was approximately 605 µM (604.9 ± 84.0 µM). In contrast, RVT was well-tolerated by HaCaT cells (showed no statistical difference from control) only at concentrations below 50 µM and demonstrated greater toxicity, with an IC50 of approximately 322 µM (322.4 ± 21.1 µM).

A similar profile was observed in L929 fibroblasts. AR26 did not impact L929 cell viability at concentrations below 200 µM, presenting an IC50 of 487.25 ± 30.1 µM. RVT, however, was tolerated only at concentrations below 50 µM, with an IC50 of 236.51 ± 18.51 µM. These data suggest that AR26 possesses a superior biocompatibility profile compared to RVT in this context.

Based on these acute cytotoxicity and biocompatibility data, the concentrations for subsequent long-term assays were strategically selected to compare the compounds at their respective minimum effective concentrations against melanoma cells: 100 µM for AR26 and 50 µM for RVT. At its selected concentration, AR26 demonstrated a superior biocompatibility profile, showing no significant impact on the viability of either HaCaT or L929. In contrast, RVT was also tolerated by HaCaT cells while inducing a slight reduction in L929 viability to approximately 87%. Notably, this value is still considered non-cytotoxic according to the ISO 10993-5 standard (>70% viability). This experimental design thus allows us to compare their effects at doses that are both

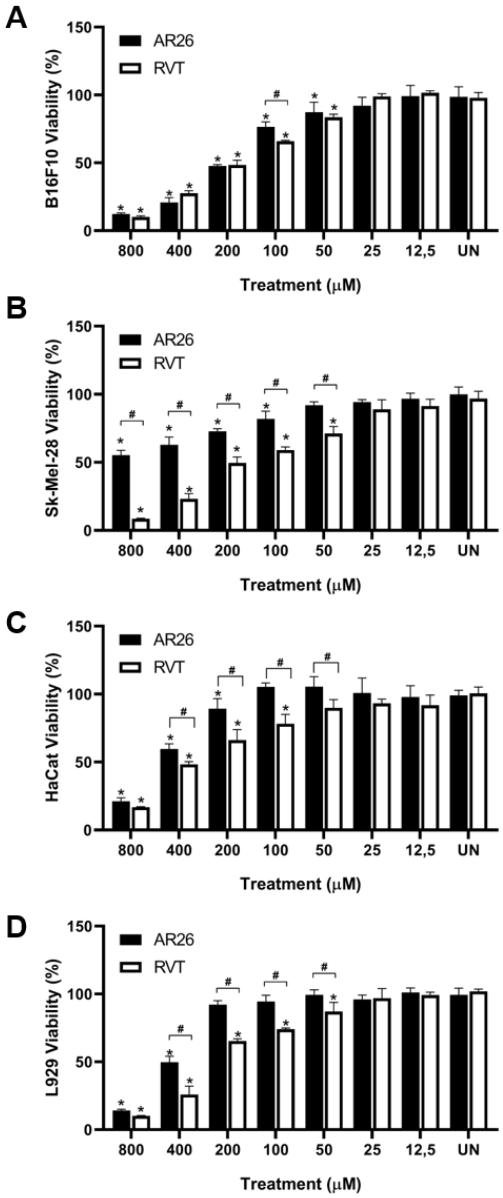

Fig. 1. AR26 exhibits a superior biocompatibility profile compared to RVT. (A, B) Acute cytotoxicity of AR26 and RVT against B16F10 (A) and SK-MEL-28 (B) melanoma cell lines. (C, D) Biocompatibility assessment in non-tumor HaCaT (C) and L929 (D) cell lines. Cells were exposed to the indicated concentrations (0–800 µM) for 24 h, and viability was determined by MTT assay. Data are presented as mean ± SD of 2 independent experiments. *p < 0.05 compared to the untreated control (UN). Statistical analysis was performed using Two-way ANOVA followed by Tukey's post hoc test.

B. AR26 inhibits migration of murine and human Melanoma cells

Tumor cell migration is a critical step in tumor invasion and metastatic dissemination [38]. We therefore evaluated the impact of AR26 on tumor cell migration using a wound-healing assay. In B16-F10 cells, non-treated controls showed approximately 80% wound closure after 24 hours (82.8% ± 15.2). Treatment with RVT (50 µM) or AR26 (100 µM) significantly reduced migration, resulting in 48.14% ± 6.9 and 49.3% ±5.4 wound closure, respectively.

In SK-MEL-28 cells, similar results were observed. Non-treated cells closed approximately 50% of the wound area after 24 hours (48.9% ± 8.3). Resveratrol-treated cells showed 17.37% ± 8.1 closure, whereas AR26-treated cells exhibited 11.7% ± 5.3 closure (Fig. 2). These findings indicate that, at their respective maximum tolerable concentrations, AR26 inhibits the migratory capacity of both murine and human melanoma cells with comparable efficacy to RVT.

This antimigratory activity is particularly significant given that cell migration represents a key determinant of metastatic potential [38]. These findings are consistent with the known ability of RVT to modulate migration through several pathways, including suppression of MMP-2/9 [39] and the regulation of epithelial-mesenchymal transition-related pathways [40–42] which are critical mediators of cancer cell invasion and dissemination. Although further studies are required, it is plausible to suppose that AR26 also acts on these or additional metastasis-linked pathways, reinforcing its therapeutic potential, particularly against metastatic tumors.

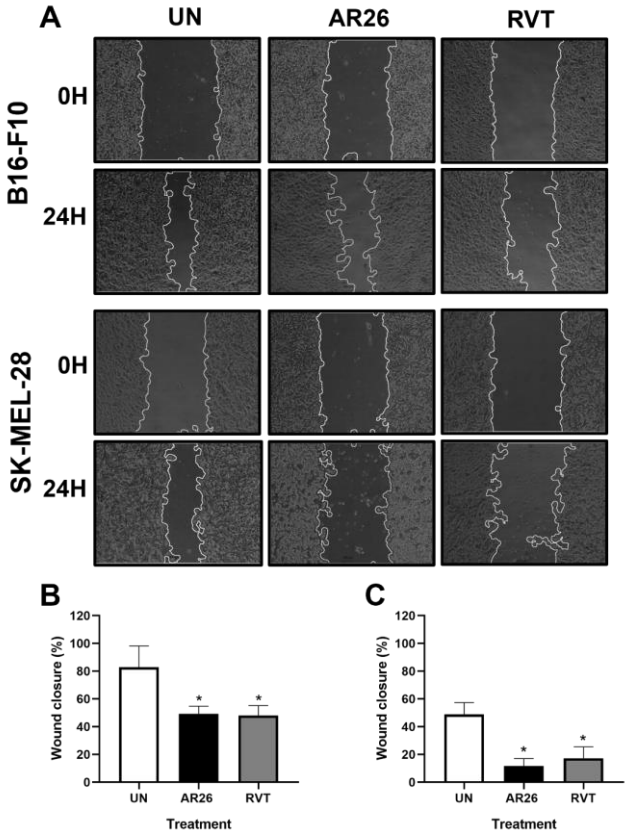

Figure 2. AR26 inhibits the migratory capacity of melanoma cells similarly to resveratrol. Representative phase-contrast images and quantitative analysis of wound-healing assay performed with murine (B16-F10) and human (SK-MEL-28) melanoma cells. Confluent monolayers were scratched and treated with AR26 (100 µM) or resveratrol (RVT, 50 µM) for 24 h in medium containing 0.5% FBS. (A) Photomicrographs show wound areas at 0 h and 24 h after treatment. (B) Quantification of wound closure (%) for B16-F10 cells. (C) Quantification of wound closure (%) for SK-Mel cells. Untreated controls (UN). Data represent mean ± SD. *p < 0.05 vs UN (one-way ANOVA followed by Tukey's post hoc test).

C. AR26 imposes a more sustained anti-proliferative effect than resveratrol

Uncontrolled proliferation is a hallmark of cancer [43], making the inhibition of cell division an important target for antitumor therapy. While short-term viability assays, such as MTT (24h) are informative for initial screening, assessing a compound's ability to sustain proliferation suppression over extended periods is crucial for predicting its therapeutic potential. We therefore used the CFSE dilution assay to track cell proliferation over 72 hours.

As shown in Figure 3, untreated cells displayed a progressive decrease in CFSE fluorescence intensity over time, consistent with active cell proliferation. In contrast, cells treated with AR26 (100 µM) or RVT (50 µM) retained significantly higher CFSE fluorescence levels at all evaluated time points, indicating reduced proliferative activity. Notably, although at 24 hours both compounds exhibited comparable effects, at the 48- and 72-hour time points, AR26 maintained a significantly stronger and more sustained inhibition in both B16-F10 and SK-MEL-28 cells compared to RVT, suggesting superior long-term efficacy.

The divergence between AR26 and RVT regarding proliferation inhibition may be attributed to the well-documented chemical instability of resveratrol, which, due to degradation, can lead to a loss of biological activity over time [44], a liability that the synthetic AR26 does not appear to share. Alternatively, AR26 may act more effectively on specific pathways, such as cell cycle regulation, inducing a more permanent arrest in contrast to the transient cytostatic effect observed with RVT. Further studies are underway to elucidate this mechanism.

Regardless of the precise mechanism, the ability to exert continuous inhibitory pressure on cell proliferation is more clinically relevant than a short-lived, acute effect, as sustained suppression is critical for triggering tumor senescence or apoptosis [45]. Therefore, the potent and sustained antiproliferative inhibition demonstrated by AR26 positions it as a more robust and viable therapeutic candidate than its parent compound.

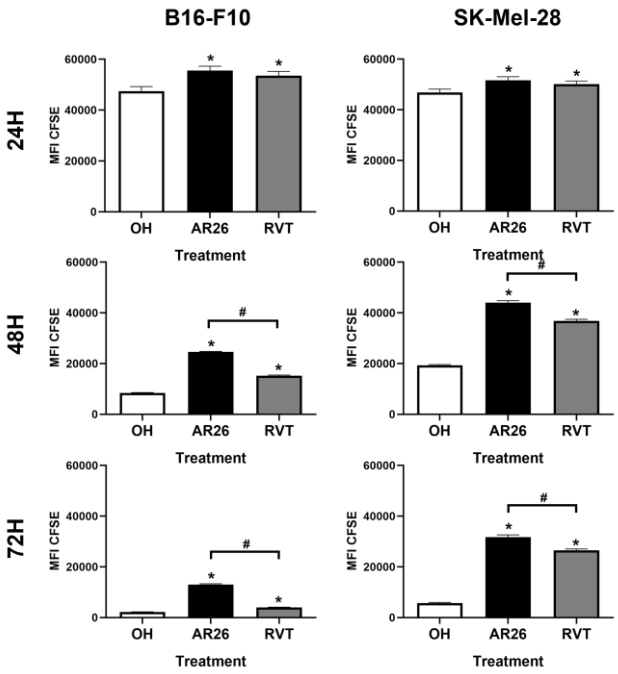

Figure 3. AR26 exerts a sustained anti-proliferative effect on melanoma cells. B16-F10 and SK-MEL-28 melanoma cells were stained with CFSE and subsequently treated with AR26 (100 µM) or resveratrol (RVT, 50 µM). Cell proliferation was assessed at 24, 48, and 72 h by measuring CFSE fluorescence dilution via flow cytometry. Data are expressed as mean fluorescence intensity (MFI) ± SD from three independent experiments. UN, untreated control. *p < 0.05 vs UN; #p < 0.05 vs RVT (one-way ANOVA followed by Tukey's post hoc test).*

D. AR26 Confers a Persistent Suppression of Tumor Cell Migration in 3D Spheroids

Finally, to assess the translational relevance of AR26 in a human context, we evaluated its efficacy using three-dimensional (3D) spheroids derived from the SK-MEL-28 human melanoma cell line. Compared with conventional two-dimensional (2D) cultures, 3D tumor spheroids more accurately recapitulate the structural complexity, intercellular interactions, and physicochemical gradients of *in vivo* tumors, including features like hypoxia and nutrient deprivation. Owing to these attributes, tumor spheroids are increasingly recognized as a physiologically relevant *in vitro* platform for anticancer drug screening [46–48].

To investigate the effects of AR26 on the growth dynamics of human melanoma spheroids, SK-MEL-28 spheroids were generated and treated with AR26 (100 µM) or RVT (50 µM) for up to 72 h. At baseline (treatment initiation), spheroids exhibited typical morphology characterized by an outer proliferative zone, a middle quiescent zone, and a central necrotic zone, consistent with previous reports [46,48,49]. During the treatment period, no significant differences were detected among the groups, indicating that neither AR26 nor RVT inhibited the growth of

established spheroids under these conditions (Fig. 4A).

Next, to assess whether AR26 could exert long-lasting effects on tumor cell migration after treatment withdrawal, the migratory potential of treated spheroids was evaluated by transferring them to adherent plates in drug-free medium. As shown in Figure 4B, C, untreated controls displayed a progressive increase in migration area, reaching an 8-fold increase over baseline at 48 h. RVT-pretreated spheroids also showed expansion, with migration areas not significantly different from untreated controls at any time point.

In contrast, AR26-pretreated spheroids exhibited markedly reduced expansion. This inhibitory effect was statistically significant when compared to both the RVT-treated group and untreated controls at 24 h and 48 h (Fig. 4B). At the 48-h endpoint, the AR26 group reached only an approximately 5-fold increase over baseline. These findings demonstrate that AR26 exerts a sustained and significant inhibitory effect on post-treatment migration, which is substantially more pronounced than that observed for RVT under these conditions.

This potent antimigratory efficacy in this more stringent setting is particularly relevant, as 3D models are known to confer drug resistance through mechanisms related to their complex architecture, physicochemical gradients, and cellular interactions [46]. Therefore, the efficacy of AR26 in this environment not only confirmed its activity against human melanoma cells but also provided evidence of its capacity to exert a durable, long-lasting biological effect after penetrating an established tumor mass. This persistent effect suggests that AR26 may induce changes that remain active even after drug withdrawal, a property with significant therapeutic implications for preventing metastatic recurrence.

Taken together, our findings indicate that AR26 acts through multiple complementary mechanisms, primarily exerting sustained antiproliferative and antimigratory effects. Notably, this potency is coupled with a superior biocompatibility profile compared to resveratrol, allowing the use of higher therapeutic concentrations (100 µM vs 50 µM). Its enhanced activity in preventing migratory outgrowth in human 3D models further positions AR26 as a promising candidate for development against metastatic cancers such as melanoma.

Future investigations should aim to delineate the molecular targets of AR26, characterize its pharmacokinetic profile, and evaluate its long-term safety and efficacy in advanced preclinical models of melanoma, including potential combination therapies. Nevertheless, the results from this study, particularly the sustained effects observed in spheroid models, provide a strong translational rationale for the continued development of AR26 as a novel therapeutic agent for targeting metastatic progression.

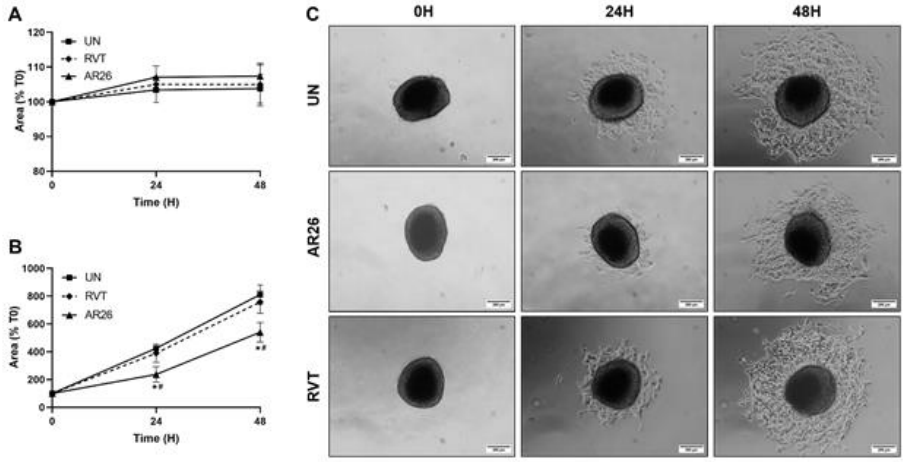

Figure 4. Effect of AR26 on SK-MEL-28 spheroid growth and post-treatment migration. (A) Spheroid growth during 72 h treatment with AR26 (100 µM) or resveratrol (RVT, 50 µM). (B) Migration area after spheroids were pretreated for 72h and transferred to adherent plates in drug-free medium. (C) Representative phase-contrast micrographs of spheroid migration at 0, 24, and 48h after treatment withdrawal. Data expressed as percentage of initial area (time 0 = 100%). UN, untreated controls. Data represent mean ± SD. *p < 0.05 vs UN; #p < 0.05 vs RVT (one-way ANOVA followed by Tukey's post hoc test).

IV. Conclusion

In summary, the synthetic resveratrol analogue AR26 demonstrated a distinct anticancer profile characterized by sustained antiproliferative and antimigratory mechanisms. Crucially, AR26 combined this efficacy with a favorable biocompatibility profile at therapeutically relevant concentrations. Furthermore, AR26 distinguished itself by maintaining long-term suppression of proliferation and effectively inhibiting migratory outgrowth from 3D melanoma spheroids. Collectively, these findings position AR26 as a promising candidate for further preclinical development targeting melanoma metastasis.

Acknowledgments

The authors are grateful to the Programa de Pós-graduação em Ciências Biológicas (PPGCBIO/UFJF), the Laboratório Integrado de Pesquisa (LIP/PPGCBIO), and Dr. Henrique Couto Teixeira for their support.

Funding

This work was supported by Fundação de Amparo à Pesquisa do Estado de Minas Gerais – FAPEMIG (APQ-02177-22, Rede Mineira de Investigação em Mucosa e Pele - RED-00096-22 and Rede Mineira de Imunobiológicos, RED-0067-23) and Conselho Nacional de Desenvolvimento Científico e Tecnológico

(CNPq). Fellowships were provided by CAPES, PROBIC/FAPEMIG and BIC/UFJF.

REFERENCES

[1] F. Bray, M. Laversanne, E. Weiderpass, and I. Soerjomataram, "The ever-increasing importance of cancer as a leading cause of premature death worldwide," *Cancer*, vol. 127, no. 16, pp. 3029–3030, Aug. 2021.

[2] F. Bray, M. Laversanne, H. Sung, J. Ferlay, R. L. Siegel, I. Soerjomataram, *et al.*, "Global cancer statistics 2022: GLOBOCAN estimates of incidence and mortality worldwide for 36 cancers in 185 countries," *CA Cancer J. Clin.*, vol. 74, no. 3, pp. 229–263, Jun. 2024.

[3] S. Chen, Z. Cao, K. Prettner, M. Kuhn, J. Yang, L. Jiao, *et al.*, "Estimates and projections of the global economic cost of 29 cancers in 204 countries and territories from 2020 to 2050," *JAMA Oncol.*, vol. 9, no. 4, pp. 465–472, Apr. 2023.

[4] D. T. Debela, S. G. Muzazu, K. D. Heraro, M. T. Ndalama, B. W. Mesele, D. C. Haile, *et al.*, "New approaches and procedures for cancer treatment: Current perspectives," *SAGE Open Med.*, vol. 9, p. 20503121211034366, Jan. 2021.

[5] B. Liu, H. Zhou, L. Tan, K. T. H. Siu, and X.-Y. Guan, "Exploring treatment options in cancer: tumor treatment strategies," *Signal Transduct. Target Ther.*, vol. 9, no. 1, p. 175, Jul. 2024.

[6] V. Jairam, V. Lee, H. S. Park, C. R. Thomas, E. R. Melnick, C. P. Gross, *et al.*, "Treatment-related complications of systemic therapy and radiotherapy," *JAMA Oncol.*, vol. 5, no. 7, p. 1028, Jul. 2019.

[7] E. M. Lee, P. Jiménez-Fonseca, R. Galán-Moral, S. Coca-Membribes, A. Fernández-Montes, E. Sorribes, *et al.*, "Toxicities and quality of life during cancer treatment in advanced solid tumors," *Curr. Oncol.*, vol. 30, no. 10, pp. 9205–9216, Oct. 2023.

[8] A. Zafar, S. Khatoon, M. J. Khan, J. Abu, and A. Naeem, "Advancements and limitations in traditional anti-cancer therapies: a comprehensive review of surgery, chemotherapy, radiation therapy and hormonal therapy," *Discov. Oncol.*, vol. 16, no. 1, p. 607, Apr. 2025.

[9] A. Zafar, M. J. Khan, J. Abu, and A. Naeem, "Revolutionizing cancer care strategies: immunotherapy, gene therapy, and molecular targeted therapy," *Mol. Biol. Rep.*, vol. 51, no. 1, p. 219, Dec. 2024.

[10] Y. Yang, Y. Chen, J. H. Wu, Y. Ren, B. Liu, Y. Zhang, *et al.*, "Targeting regulated cell death with plant natural compounds for cancer therapy," *Phytother. Res.*, vol. 37, no. 4, pp. 1488–1525, Apr. 2023.

[11] B. Tian and J. Liu, "Resveratrol: a review of plant sources, synthesis, stability, modification and food application," *J. Sci. Food Agric.*, vol. 100, no. 4, pp. 1392–1404, Mar. 2020.

[12] J. H. Holthoff, K. A. Woodling, D. R. Doerge, S. T. Burns, J. A. Hinson, and P. R. Mayeux, "Resveratrol, a dietary polyphenolic phytoalexin, is a functional scavenger of peroxynitrite," *Biochem. Pharmacol.*, vol. 80, no. 8, pp. 1260–1265, Oct. 2010.

[13] X.-L. Bi, J.-Y. Yang, Y.-X. Dong, J.-M. Wang, Y.-H. Cui, T. Ikeshima, *et al.*, "Resveratrol inhibits nitric oxide and TNF-α production by lipopolysaccharide-activated microglia," *Int. Immunopharmacol.*, vol. 5, no. 1, pp. 185–193, Jan. 2005.

[14] X. Gao, Y.-X. Xu, N. Janakiraman, R. A. Chapman, and S. C. Gautam, "Immunomodulatory activity of resveratrol: suppression of lymphocyte proliferation and cytokine production," *Biochem. Pharmacol.*, vol. 62, no. 9, pp. 1299–1308, Nov. 2001.

[15] X. Gao, D. Deeb, J. C. Media, G. Divine, H. Jiang, R. A. Chapman, *et al.*, "Immunomodulatory activity of resveratrol: discrepant in vitro and in vivo immunological effects," *Biochem. Pharmacol.*, vol. 66, no. 12, pp. 2427–2435, Dec. 2003.

[16] D.-I. Cho, N.-Y. Koo, W.-J. Chung, T.-S. Kim, S.-Y. Ryu, S.-Y. Im, *et al.*, "Effects of resveratrol-related hydroxystilbenes on nitric oxide production in macrophage cells," *Life Sci.*, vol. 71, no. 17, pp. 2071–2082, Sep. 2002.

[17] K. B. Harikumar, A. B. Kunnumakkara, G. Sethi, P. Diagaradjane, P. Anand, M. K. Pandey, *et al.*, "Resveratrol enhances antitumor activity of gemcitabine in vitro and in an orthotopic mouse model," *Int. J. Cancer*, vol. 127, no. 2, pp. 257–268, Jul. 2010.

[18] A. Wahab, K. Gao, C. Jia, F. Zhang, G. Tian, G. Murtaza, *et al.*, "Significance of resveratrol in clinical management of chronic diseases," *Molecules*, vol. 22, no. 8, p. 1329, Aug. 2017.

[19] Y. Yang, Y. Chang, P. Huang, G. Chiou, L. Tseng, S. Chiou, *et al.*, "Resveratrol suppresses tumorigenicity and enhances radiosensitivity in primary glioblastoma initiating cells," *J. Cell. Physiol.*, vol. 227, no. 3, pp. 976–993, Mar. 2012.

[20] H.-T. Yin, Q.-Z. Tian, L. Guan, Y. Zhou, X.-E. Huang, and H. Zhang, "In vitro and in vivo evaluation of the antitumor efficiency of resveratrol against lung cancer," *Asian Pac. J. Cancer Prev.*, vol. 14, no. 3, pp. 1703–1706, Mar. 2013.

[21] L. Q. Trung, J. L. Espinoza, D. T. An, N. H. Viet, K. Shimoda, and S. Nakao, "Resveratrol selectively induces apoptosis in malignant cells with the JAK2V617F mutation," *Mol. Nutr. Food Res.*, vol. 59, no. 11, pp. 2143–2154, Nov. 2015.

[22] M. Jang, L. Cai, G. O. Udeani, K. V. Slowing, C. F. Thomas, C. W. W. Beecher, *et al.*, "Cancer chemopreventive activity of resveratrol, a natural

product derived from grapes," *Science*, vol. 275, no. 5297, pp. 218–220, Jan. 1997.

[23] L. G. Carter, J. A. D'Orazio, and K. J. Pearson, "Resveratrol and cancer: focus on in vivo evidence," *Endocr. Relat. Cancer*, vol. 21, no. 3, pp. R209–R225, Jun. 2014.

[24] M. Yousef, I. Vlachogiannis, and E. Tsiani, "Effects of resveratrol against lung cancer: in vitro and in vivo studies," *Nutrients*, vol. 9, no. 11, p. 1231, Nov. 2017.

[25] T. Hsieh, C. Wong, D. J. Bennett, and J. M. Wu, "Regulation of p53 and cell proliferation by resveratrol and its derivatives," *Int. J. Cancer*, vol. 129, no. 11, pp. 2732–2743, Dec. 2011.

[26] K. Bove, D. W. Lincoln, and M.-F. Tsan, "Effect of resveratrol on growth of 4T1 breast cancer cells in vitro and in vivo," *Biochem. Biophys. Res. Commun.*, vol. 291, no. 4, pp. 1001–1005, Mar. 2002.

[27] F. De Amicis, F. Giordano, A. Vivacqua, M. Pellegrino, M. L. Panno, D. Tramontano, *et al.*, "Resveratrol, through NF-Y/p53/Sin3/HDAC1 complex phosphorylation, inhibits estrogen receptor α gene expression via p38MAPK/CK2 signaling in human breast cancer cells," *FASEB J.*, vol. 25, no. 10, pp. 3695–3707, Oct. 2011.

[28] V. M. Adhami, F. Afaq, and N. Ahmad, "Suppression of ultraviolet B exposure-mediated activation of NF-κB in normal human keratinocytes by resveratrol," *Neoplasia*, vol. 5, no. 1, pp. 74–82, Jan. 2003.

[29] X. Yu, Z. Sun, S. Nie, T. Zhang, and H. Lu, "Effects of resveratrol on mouse B16 melanoma cell proliferation through the SHCBP1-ERK1/2 signaling pathway," *Molecules*, vol. 28, no. 22, p. 7614, Nov. 2023.

[30] M. Y. Zamanian, T. Shahbazi, S. W. Kazmi, B. M. Hussien, A. Sharma, M. T. Qasim, *et al.*, "Effects of resveratrol on nonmelanoma skin cancer: A comprehensive review," *Food Sci. Nutr.*, vol. 12, no. 11, pp. 8825–8845, Nov. 2024.

[31] F. Casanova, J. Quarti, D. C. F. Da Costa, C. A. Ramos, J. L. Da Silva, and E. Fialho, "Resveratrol chemosensitizes breast cancer cells to melphalan by cell cycle arrest," *J. Cell. Biochem.*, vol. 113, no. 8, pp. 2586–2596, Aug. 2012.

[32] G. A. Abdel-Latif, A. M. Al-Abd, M. G. Tadros, F. A. Al-Abbasi, A. E. Khalifa, and A. B. Abdel-Naim, "The chemomodulatory effects of resveratrol and didox on herceptin cytotoxicity in breast cancer cell lines," *Sci. Rep.*, vol. 5, no. 1, p. 12054, Jul. 2015.

[33] X.-P. Shi, S. Miao, Y. Wu, W. Zhang, X.-F. Zhang, H.-Z. Ma, *et al.*, "Resveratrol sensitizes tamoxifen in anti-estrogen-resistant breast cancer cells with epithelial–mesenchymal transition features," *Int. J. Mol. Sci.*, vol. 14, no. 8, pp. 15655–15668, Jul. 2013.

[34] T. Walle, F. Hsieh, M. H. DeLegge, J. E. Oatis, and U. K. Walle, "High absorption but very low bioavailability of oral resveratrol in humans," *Drug Metab. Dispos.*, vol. 32, no. 12, pp. 1377–1382, Dec. 2004.

[35] D. C. Zimmermann-Franco, B. Esteves, L. M. Lacerda, I. D. O. Souza, J. A. D. Santos, N. D. C. C. Pinto, *et al.*, "In vitro and in vivo anti-inflammatory properties of imine resveratrol analogues," *Bioorg. Med. Chem.*, vol. 26, no. 17, pp. 4898–4906, Sep. 2018.

[36] S. H. Jeong, I. S. Song, H. K. Kim, S. R. Lee, S. Song, H. Suh, *et al.*, "An analogue of resveratrol HS-1793 exhibits anticancer activity against MCF-7 cells via inhibition of mitochondrial biogenesis gene expression," *Mol. Cells*, vol. 34, no. 4, pp. 357–366, Oct. 2012.

[37] L. M. R. Antinarelli, R. S. Meinel, E. A. F. Coelho, A. D. Da Silva, and E. S. Coimbra, "Resveratrol analogues present effective antileishmanial activity against promastigotes and amastigotes by multitarget action," *J. Pharm. Pharmacol.*, vol. 71, no. 12, pp. 1854–1863, Dec. 2019.

[38] J. J. Bravo-Cordero, L. Hodgson, and J. Condeelis, "Directed cell invasion and migration during metastasis," *Curr. Opin. Cell Biol.*, vol. 24, no. 2, pp. 277–283, Apr. 2012.

[39] W. Chang, C. Tsai, J. Yang, Y. Hsu, L. Shih, H. Chiu, *et al.*, "Resveratrol inhibited metastatic behaviors of cisplatin-resistant human oral cancer cells via ERK/p38 phosphorylation and MMP-2/9 suppression," *J. Food Biochem.*, vol. 45, no. 6, Jun. 2021.

[40] W. Li, J. Ma, Q. Ma, B. Li, L. Han, J. Liu, *et al.*, "Resveratrol inhibits epithelial–mesenchymal transition of pancreatic cancer cells via suppression of the PI3K/Akt/NF-κB pathway," *Curr. Med. Chem.*, vol. 20, no. 33, pp. 4185–4194, Sep. 2013.

[41] M.-C. Chen, W.-W. Chang, Y.-D. Kuan, S.-T. Lin, H.-C. Hsu, and C.-H. Lee, "Resveratrol inhibits LPS-induced epithelial–mesenchymal transition in a mouse melanoma model," *Innate Immun.*, vol. 18, no. 5, pp. 685–693, Oct. 2012.

[42] L. Yuan, M. Zhou, D. Huang, H. Wasan, K. Zhang, L. Sun, *et al.*, "Resveratrol inhibits invasion and metastasis of colon cancer through reversal of epithelial–mesenchymal transition via the AKT/GSK-3β/Snail signaling pathway," *Mol. Med. Rep.*, 2019.

[43] D. Hanahan, "Hallmarks of cancer: New dimensions," *Cancer Discov.*, vol. 12, no. 1, pp. 31–46, Jan. 2022.

[44] Š. Zupančič, Z. Lavrič, and J. Kristl, "Stability and solubility of trans-resveratrol are strongly influenced by pH and temperature," *Eur. J. Pharm. Biopharm.*, vol. 93, pp. 196–204, Jun. 2015.

[45] T. Otto and P. Sicinski, “Cell cycle proteins as promising targets in cancer therapy,” *Nat. Rev. Cancer*, vol. 17, no. 2, pp. 93–115, Feb. 2017.

[46] R. Edmondson, J. J. Broglie, A. F. Adcock, and L. Yang, “Three-dimensional cell culture systems and their applications in drug discovery and cell-based biosensors,” *Assay Drug Dev. Technol.*, vol. 12, no. 4, pp. 207–218, May 2014.

[47] Y. Imamura, T. Mukohara, Y. Shimono, Y. Funakoshi, N. Chayahara, M. Toyoda, *et al.*, “Comparison of 2D- and 3D-culture models as drug-testing platforms in breast cancer,” *Oncol. Rep.*, vol. 33, no. 4, pp. 1837–1843, Apr. 2015.

[48] M. Zanoni, F. Piccinini, C. Arienti, A. Zamagni, S. Santi, R. Polico, *et al.*, “3D tumor spheroid models for in vitro therapeutic screening: A systematic approach to enhance biological relevance,” *Sci. Rep.*, vol. 6, no. 1, p. 19103, Jan. 2016.

[49] B. Pinto, A. C. Henriques, P. M. A. Silva, and H. Bousbaa, “Three-dimensional spheroids as in vitro preclinical models for cancer research,” *Pharmaceutics*, vol. 12, no. 12, p. 1186, Dec. 2020.